ining gene expression using DNA microarrays will allow us to elucidate the life-span promoting mechanism of *Rhei Rhizoma* at the molecular level.

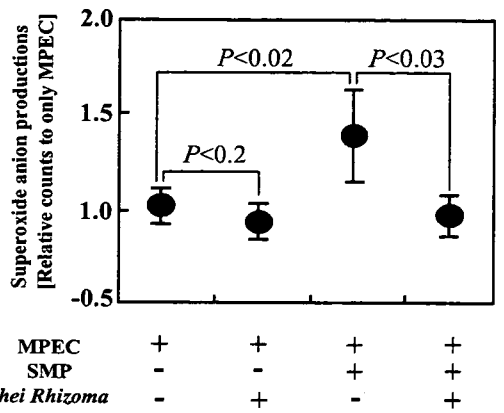

Fig. 6. Superoxide anion production. Each column with error bars indicates the mean value with the standard deviation from three separate experiments.

Acknowledgements

This work is supported by grant-in-aid for Aging Research from the Ministry of Health, Labor and Welfare, Japan.

References

Adachi, H., Fujiwara,Y., and Ishii, N. (1998) Effects of oxygen on protein carbonyl and aging in *Caenorhabditis elegans* mutants with long (*age-1*) and short (*mev-1*) life spans, *J. Geront.: Biol. Sc.i*,, 53, B240-B244.

Brenner, S. (1974) The genetics of *Caenorhabditis elegans*, *Genetics*, 77, 71-94.

Collins, A.R., Duthie, S.J., Pillion, L., Gedik, C.M., Vaughan, N., and Wood, S.G. (1997) Oxidative DNA damage in human cells: The influence of antioxidants and DNA repair, *Biochem. Soc. Transact.*, 25, 326-331.

Emmons, S.W., Klass, M.R., and Hirsh, D. (1979) Analysis of the constancy of DNA sequenced during development and evolution of the nematode *Caenorhabditis elegans*, *Proc. Natl. Acad. Sci. USA*, 76, 1333-1337.

Finkel, T., and Holbrook, N. J. (2000) Oxidants, oxidative stress and the biology of ageing, *Nature*, 408, 239-247.

Haenold, R., Wassef, D.M., Heinemann, S.H., and Hoshi, T. (2005) Oxidative damage, aging and anti-aging strategies, *Age*, 27, 183-199.

Honda, S., Ishii, N., Suzuki, K. and Matsuo, M. (1993) Oxygen-dependent perturbation of life span and aging rate in the nematode, *J. Geront.: Biol. Sc.i*, 48, B57-B61.

Hosokawa, H., Ishii, N., Ishida, H., Ichimori, K., Nakazawa, H., and Suzuki, K. (1994) Rapid accumulation of fluorescent material with aging in an oxygen-sensitive mutant *mev-1* of *Caenorhabditis elegans*, *Mech. Ageing Dev.*, 74, 161-170.

Houthoofd, K., Braeckman, B.P., Lenaerts, I., Brys, K., De Vreese, A., Van Eygen, S., and Vanfleteren, J.R. (2002) No reduction of metabolic rate in food restricted *Caenorhabditis elegans*, *Exp. Geront.*, 37, 1357-1367.

Ishii, N., Fujii, M., Hartman, P.S., Tsuda, M., Yasuda, K., Senoo-Matsuda, N., Yanase, S., Ayusawa, D., and Suzuki, K. (1998) A mutation in succinate dehydrogenase cytochrome *b* causes oxidative stress and ageing in nematodes, *Nature*, 394, 6694-6697.

Ishii, N., Goto, S., and Hartman, P.S. (2002) Protein oxidation during aging of the nematode *Caenorhabditis elegans*, *Free Radic. Biol. Med.*, 33, 1021-1025.

Ishii, N., Senoo-Matsuda, N., Miyake, K., Yasuda, K., Ishii, T., Hartman, P.S., and Furukawa, S. (2004) Coenzyme Q_{10} can prolong *C. elegans* lifespan by lowering oxidative stress, *Mech. Ageing Dev.*, 125, 41-46.

Jansson, H.B., Jeyaprakash, A., Marban-Mendoza, N., and Zuckerman, B.M. (1986) *Caenorhabditis elegans*: comparisons of chemotactic behavior from monoxenic and axenic culture, *Exp. Parasitol.*, 61, 369-372.

Jewitt, N., Anthony, P., Lowe, K.C., and De Pomerai, D.I. (1999) Oxygenated perfluorocarbon promotes nematode growth and stress-sensitivity in a two-phase liquid culture system, *Enzyme Microbial. Tech*, 25, 349-356.

Kishikawa, M., and Sakae, M. (1997) Herbal medi-

cine and the study of aging in senescence-accelerated mice (SAMP1TA/Ngs), *Exp. Geront.*, 32, 229-242.

Klass, M. (1977) Aging in the nematode *Caenorhabditis elegans*: Major biological and envieonmental factors influencing life span, *Mech. Ageing Dev.*, 6, 413-429.

Klass, M., and Hirsh, D. (1976) Non-ageing developmental variant of *Caenorhabditis elegans*, *Nature*, 260, 523-525.

Lenaz, G., (1998) Role of mitochondria in oxidative stress and ageing, *Biochim. Biophys. Acta.*, 1366, 53-67.

Lewis J.A., and Fleming. J.T. (1995) Basic culture method: Modern Biological Analysis of an Organism: Method in Cell Biology, eds. by H. F. Epstein and D.C. Ashakes, pp.3-29, Academic Press U.K.

Luo, Y. (2006) Alzheimer's disease, the nematode *Caenorhabditis elegans*, and ginkgo biloba leaf extract, *Life Sci.*, 78, 2066-2072.

Melov, S., Ravenscroft, J., Malik, S., Gill, M.S., Waker, D.W., Clayton, P.E., Wallace, D.C., Malfroy, B., Doctrow, S.R., and Lithgow, G.J. (2000) Extension of life-span with superoxide dismutase/catalase mimietics, *Science*, 289, 1567-1569.

Mitchell, D.H., Stiles, J.W., Santelli, J., and Rad Sanadi, D. (1979) Synchronous growth and aging of *Caenorhabditis elegans* in the presence of fluorodeoxyuridine, *J. Geront.*, 35, 28-36.

Petrascheck, M., Ye, X. and Buck, L.B. (2007) An antidepressant that extends lifespan in adult *Caenorhabditis elegans*, *Nature*, 450, 553-556.

Raha, S., and Robinson, B. H. (2000) Mitochondria, oxygen free radicals, disease and ageing, *Trends Biochem. Sci*,, 25, 502-508.

Roberts, T.M., and Ward, S. (1982) Membrane flow during nematode spermigenesis, *J. Cell Biol.*, 92, 113-120.

Shimomura, O., Wu, C., Murai, A., and Nakamura, H. (1998) Evaluation of five imidazopyrazinone-type chemiluminescent superoxide probes and their application to the measurement of superoxide anion generated by Listeria monocytogenes, *Anal. Biochem.*, 258, 230-235.

Sulston J.E., and Brenner S. (1974) The DNA of *Caenorhabditis elegans*, *Genetics*, 77, 95-104.

Sulston, J.E. (1988) Cell lineage. in The nematode *Caenorhabditis elelgans*, ed. by W. B. Wood, pp.123-155, Cold Spring Harbor Laboratory N.Y.

Sulston, J.E., and Horvitz, H.R. (1977) Post-embryonic cell lineages of the nematode *Caenorhabditis elegans*, *Dev. Biol.*, 56, 110-156.

The C. elegans Sequencing Consortium. (1988) Genome sequence of the nematode *C. elegans*: a platform for investigating biology, *Science*, 282, 2012–2018.

Turrens, J.F., Alexandre, A., and Lehninger, A.L. (1985) Ubisemiquinone is the electron donor for superoxide formation by complex III of heart mitochondria, *Arch. Biochem. Biophys.*, 237, 408-414.

Vanfleteren, J.R. (1980) Nematods as nutritional models. in Nematodes as biological models, Volume 2: Aging and other model systems, ed. by B. M. Zuckerman, pp.47-49, Academic Press N.Y.

Vuillaume, M. (1987) Reduced oxygen species, mutation, induction and cancer initiation, *Mutat. Res.*, 186, 43-72.

Wood, W.B., (1988) Embryology, in The nematode *Caenorhabditis elelgans*, by W. B. Wood, pp. 215-241, Cold Spring Harbor Laboratory N.Y.

Yasuda, K., Ishii, T., Suda, H., Akatsuka, A., Hartman, P.S., Goto, S., Miyazawa, M., and Ishii, N. (2006) Age-related changes of mitochondrial structure and function in *Caenorhabditis elegans*, *Mech. Ageing Dev.*, 127, 763-770.

Corresponding author:
Naoaki Ishii
Department of Molecular Life Science
Tokai University School of Medicine
143 Shimokasuya, Isehara, Kanagawa 259-1193
Japan
Tel: +81-463-93-1121x2651
Fax: +81-463-94-8884
E-mail: nishii@is.icc.u-tokai.ac.jp

Geriatr Gerontol Int 2007; 7: 316–325

REVIEW ARTICLE

Significance of SMP30 in gerontology

Akihito Ishigami and Naoki Maruyama

Aging Regulation, Tokyo Metropolitan Institute of Gerontology, Tokyo, Japan

The expression of senescence marker protein-30 (SMP30) was discovered by proteomic analysis. The fact that this molecule's structure is so highly conserved among numerous species strongly suggests that the age-dependent decrease of SMP30 may contribute to senescence. Research that targeted the *SMP30* gene showed deterioration in several organs accompanied by a shortened life span. We then identified SMP30 as gluconolactonase (GNL). The lactonase reaction with L-gulono-γ-lactone is the penultimate step in vitamin C (L-ascorbic acid) biosynthesis. Our discovery has opened the door to a new aspect of aging studies.

Keywords: aging model, apoptosis, calorie restriction, gluconolactonase, SMP30, vitamin C.

Introduction

Senescence processes are time-dependent, deteriorative and functional changes in all living bodies. After middle age, we humans daily experience loss functions of several organs. However, the degree of deterioration varies in each individual. This variation suggests that senescence is pleiotropic, attributable to numerous candidate molecules. Therefore, to evaluate the extent of senescence, a convenient marker is an absolute requirement. Some modified substances such as 8-oxo-7,8-dihydro-2′-deoxyguanosine (8-oxodG) or a hormone like DHEA-S have been reported as useful for this purpose.[1,2] However, these markers are not directly encoded by the genome. Furthermore, these substances are disadvantageous for modifying a gene to establish a model of aging. Recent advances in gene technology have now provided several useful mouse strains for aging research. In Japan, some well-known aging-prone murine strains (i.e. senescence-accelerated mouse, klotho mice) are presently available.[3,4] Although experiments with those strains have revealed useful data about senescence, they do not cover the whole spectrum in aging research. In this review, we introduce the molecules now considered critical for advancing this area of research and a widely applicable strain of mice.

Accepted for publication 22 April 2007.

Correspondence: Dr Akihito Ishigami PhD, Aging Regulation, Tokyo Metropolitan Institute of Gerontology, 35-2 Sakae-cho, Itabashi-ku, Tokyo 173-0015, Japan. Email: ishigami@tmig.or.jp

Discovery of senescence marker protein-30

In 1991, to search for the molecular abnormality at work in the aging process, we surveyed age-associated changes in soluble proteins from rat livers by using proteomic analysis and two-dimensional gel electrophoresis (2D-PAGE). Thereby, we detected and isolated a novel rat liver protein, which as first calculated had a molecular weight of 30 kDa according to the commercial molecular weight markers then available. Because the amounts of this protein decreased androgen-independently with aging, we named it senescence marker protein-30 (SMP30).[5] That designation of SMP30 was accurate until, in more sensitive resolutions, the mass of a SMP molecule proved to be 34 kDa (Fig. 1). However, the earlier name remained in use.

The next step was to prepare an antiserum to SMP30, which was applied to localize SMP30 and identified this protein most prominently in the liver and kidneys among the various organs tested (Fig. 2).[6] Subsequently, we isolated and characterized two cDNA clones encoding rat SMP30.[7] The open reading frame consisting of 897 bp encoded 299 amino acids. The estimated molecular weight and pI of the deduced polypeptide were 33 387 and 5.1, respectively. Genomic Southern hybridization analysis demonstrated that SMP30 was

 doi: 10.1111/j.1447-0594.2007.00420.x

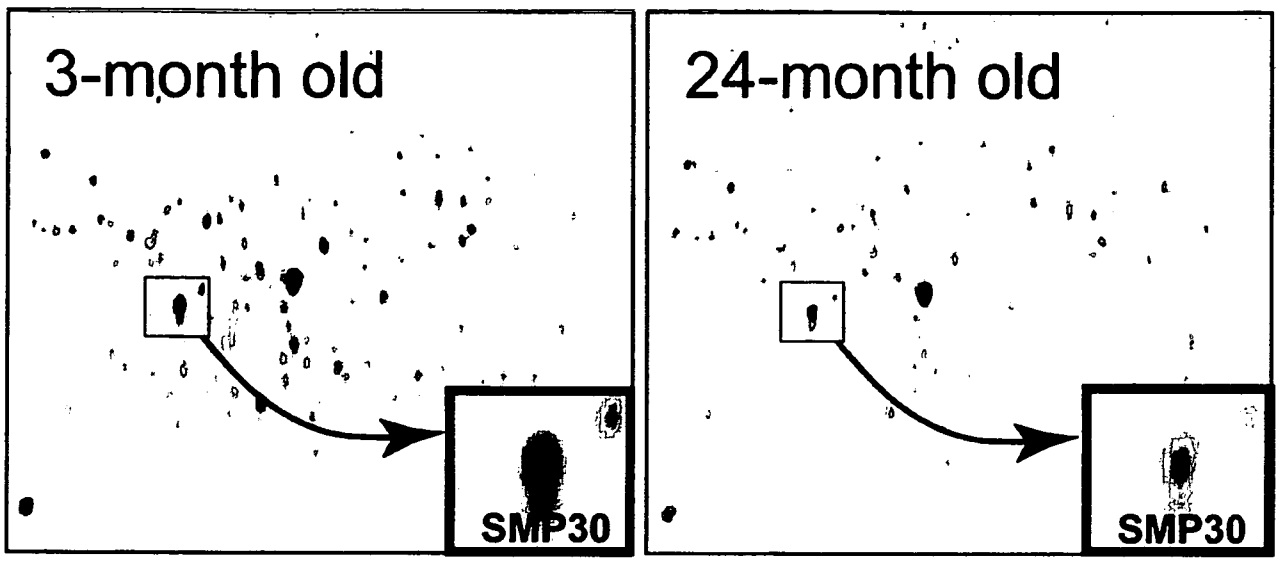

Figure 1 Proteomic profile of senescence marker protein-30 (SMP30) in soluble proteins from 3- and 24-month-old rats. SMP30 is identified as a molecule mass of 34 kDa. Amounts of this protein decrease with aging in an androgen-independent manner.

widely conserved among higher animals. At that time, a computer-assisted homology analysis of nucleic acid and protein databases revealed no marked homology with other known proteins. Therefore, SMP30 seemed to be a novel protein. Additionally, we cloned human SMP30 and documented its 88.6% homology with rat SMP30.[8] The results of regional mapping using a panel of 11 rodent–human somatic hybrids indicated that the gene is located in the p11.3–q11.2 segment of the X chromosome.[8] Analysis of the murine genomic clone revealed that the *SMP30* gene was organized into seven exons and six introns, spanning approximately 17.5 kb[9] Again, the accumulated genomic information showed that the *SMP30* gene is highly conserved among numerous animal species, and this finding was expanded to include non-vertebrates.[10,11] These results indicate the critical biological functions of SMP30.

Functions of SMP30

At the time we discovered SMP30, no functional domain was recognized in the entire amino acid sequence. Subsequently, another research group reported a calcium-binding protein identified with SMP30. However, our purified rat SMP30 and the *Sarcophaga* homolog (anterior fat protein, AFP) failed to show calcium-binding activity.[11,12]

In our laboratory, the evaluation of SMP30 continued for the purpose of examining its possible function in calcium homeostasis.[13,14] Our results established that HepG2 (HepG2/SMP30), a human hepatoma cell line, expressed large amounts of SMP30 after transfection with human cDNA. An investigation followed of the cytosolic free Ca^{2+} concentration ($[Ca^{2+}]i$) and the Na^{+}-independent Ca^{2+} efflux from these cells after extracellular adenosine triphosphate (ATP) stimulation. Although stimulation with ATP caused a transient increase of $[Ca^{2+}]i$ in both HepG2/SMP30 and mock-transfected HepG2 cells, the rate of $(Ca^{2+})i$ decrease after that peak was enhanced twofold by transfection with human SMP30 cDNA. Correspondingly, Ca^{2+} efflux was significantly increased in transfected HepG2/SMP30 cells compared with mock transfectants. In addition, more SMP30 transfectants survived than mock transfectants when cell death was induced by Ca^{2+} ionophore treatment. These results suggested that SMP30 regulates $(Ca^{2+})i$ by modulating the Ca^{2+}-pumping activity on plasma membranes. Therefore, downregulation of SMP30 during aging may contribute to the deterioration of cellular functions.

In 1999, a report on the function of SMP30 appeared in which Billecke *et al.* characterized a novel soluble protein from the mouse liver as having enzymic activity; that is, hydrolysis of diisopropyl phosphorofluoridate (DFP).[15] This molecule also hydrolyzes sarin, soman and tabun, the poisons famously used by Japanese terrorists. However, it lacks paraoxonase and arylesterase activities with respect to paraoxon and phenyl acetate, respectively. Subsequent amino acid sequencing of the purified DFPase showed it to be identical with SMP30.[16] Thus, SMP30 was classified as an enzyme. However, the substrates used in those studies were artificial chemicals developed after World War I.

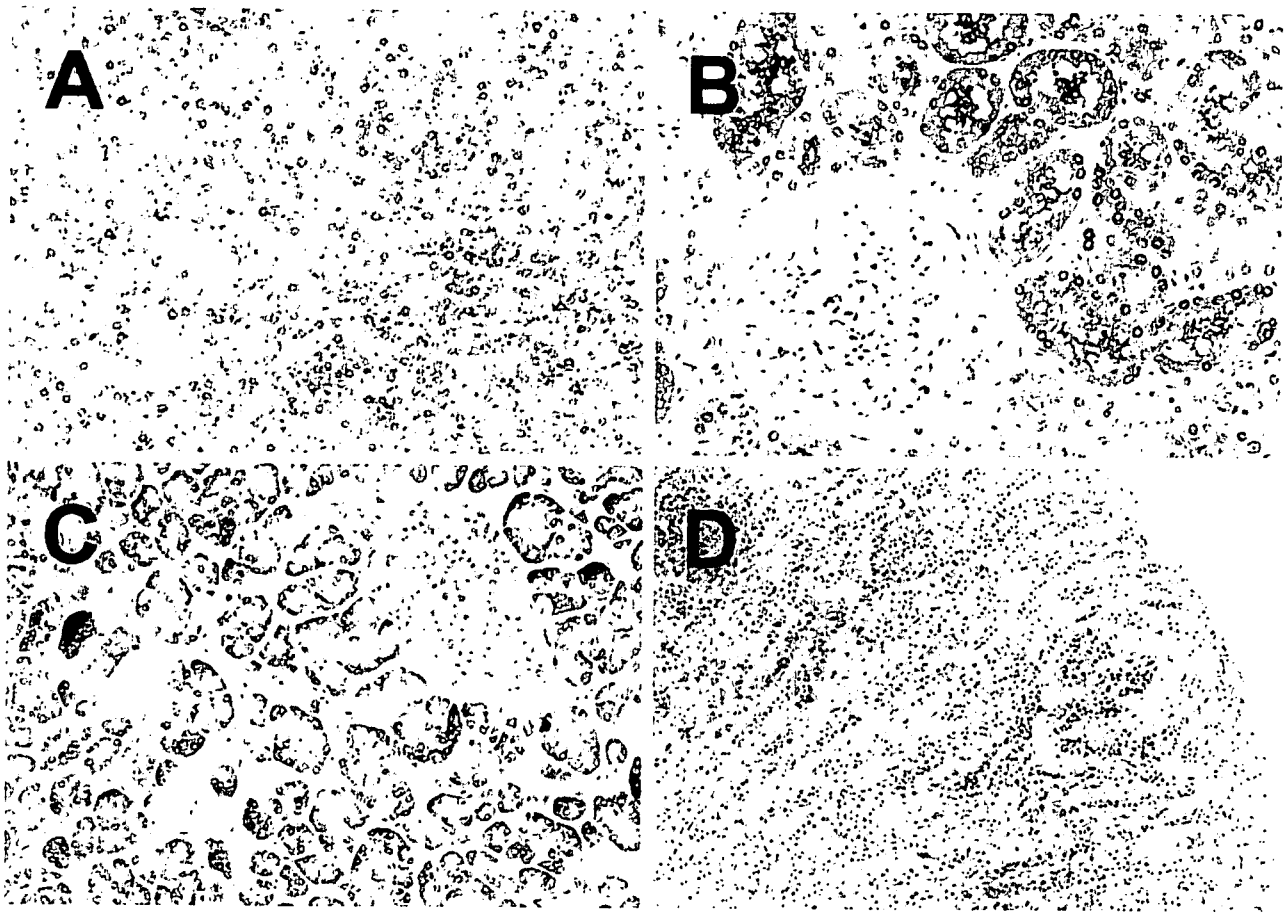

Figure 2 SMP30 expression in human organs. (a) Liver; SMP30 is expressed in parenchymal cells. (b) Kidney; SMP30 is abundant in proximal tubular cells. Localization of SMP30 at the brush border is prominent. (c) Pancreatic; acinal and ductal cells are positive for SMP30. No positive staining occurs in islets of Langerhans. (d) Adrenals; SMP30 is markedly expressed in fasciculata cells of the adrenal cortex.

We also characterized the nature of SMP30 as an organophosphatase.[12] Despite the sequence similarity between SMP30 and a serum paraoxonase (PON), the inability of SMP30 to hydrolyze PON-specific substrates such as paraoxon, dihydrocoumarin, γ-nonalactone and δ-dodecanolactone indicate that SMP30 is distinct from the PON family. The livers from normal mice contained readily detectable DFPase activity, whereas no such enzyme activity was found in livers from mice lacking SMP30. Moreover, the hepatocytes of mice lacking SMP30 were far more susceptible to DFP-induced cytotoxicity than those from the normal mice. This phenomenon accounts for the functional decrease of detoxification in elderly people.

The first report of a natural substrate for SMP30 came from Gomi *et al.*, who identified a SMP30 homolog designated as the luciferin-regeneration enzyme (LRE) in fireflies (*Photius pyralis*).[17,18] LRE converts oxyluciferin to luciferin via an intermediary substance. The deduced amino acid sequence based on cDNA analysis showed at most a 39% identity with insect AFP and mammalian SMP30. However, only 1% of LRE is expressed in the lanterns of fireflies. Despite this possible link to LRE, no genuine function of SMP30 in the whole body has yet been clarified.

Recently, we found a homology between rat SMP30 and two kinds of bacterial gluconolactonase (GNL: EC 3.1.1.17) derived from *Nostoc punctiforme* and *Zymomonas mobilis*.[19] Through subsequent biochemical study, we identified SMP30 as the lactone-hydrolyzing enzyme GNL of animal species.[20] SMP30 purified from the rat liver had lactonase activity toward the aldonolactones D- and L-glucono-δ-lactone, D- and L-gulono-γ-lactone, and D- and L-galactono-γ-lactone, with a requirement for Zn^{2+} or Mn^{2+} as a cofactor. Furthermore, in SMP30-knockout mice, no GNL activity was detectable in the liver. Thus, we concluded that SMP30 is a unique GNL in the liver. In the first report on the discovery of GNL in higher animal species, its molecules were not described in detail.[21]

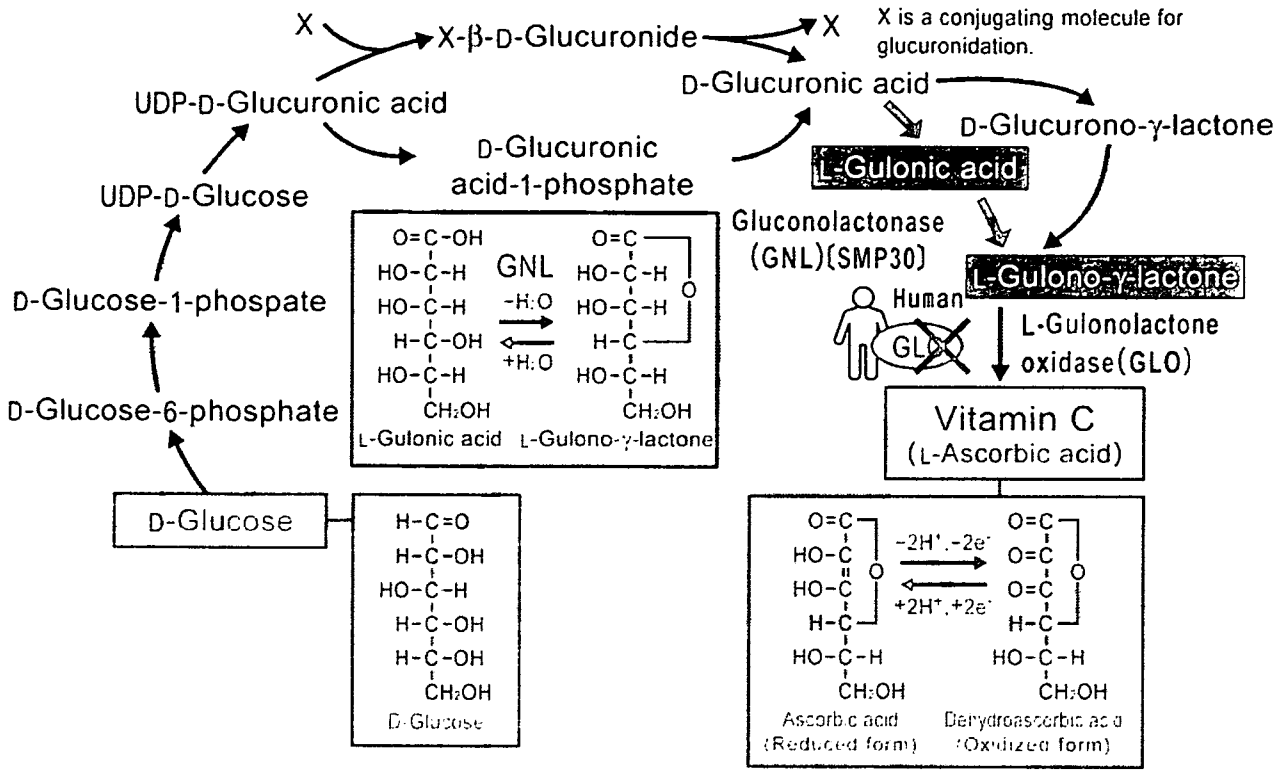

Figure 3 Vitamin C biosynthesis pathway. The pathway from D-glucose to L-gulonic acid is shared with that of early steps in the uronic acid cycle. X is a conjugating molecule for glucuronidation. SMP30 is a gluconolactonase (GNL), which catalyzes from L-gulonic acid to L-gulono-γ-lactone. In humans, L-gulonolactone oxidase (GLO) is absent because of mutation.

The lactonase reaction with L-gulono-γ-lactone is the penultimate step in vitamin C (L-ascorbic acid) biosynthesis (Fig. 3). SMP30-knockout mice fed a vitamin C-deficient diet did not thrive. They displayed symptoms of scurvy such as bone fracture and rachitic rosary and then died by 135 days after starting this vitamin C-deficient diet. The vitamin C levels in their livers and kidneys at the time of death were less than 1.6% of those in wild-type control mice. In addition, by using SMP30-knockout mice, we demonstrated that the alternative pathway of vitamin C synthesis involving D-glucurono-γ-lactone operates *in vivo*, although its flux is fairly small.

Additional and unique functions of SMP30 have also been reported. In experiments with the aforementioned HepG2 (HepG2/SMP30) cells expressed large amounts of SMP30, we observed a slower rate and decreased amount of DNA synthesis than in control HepG2 cells (mock transfected with pcDNA3 vector only).

Ultrastructural studies by scanning electron microscopy revealed numerous microvilli covering the surfaces of HepG2/SMP30 cells, whereas few microvilli appeared on control HepG2 cells.[22] Subsequently, transmission electron microscopy disclosed groups of HepG2/SMP30 cells with bile canaliculi and specialized adhesion contacts, such as tight junctions and desmosomes, at interplasmic membranes. However, in controls, units of only two cells were seen, and these lacked specialized adhesion junctions. Moesin,[23] which plays a crucial role in the formation of microvilli structures, and ZO-1,[24] which concentrated in tight junctions and adherence junctions located at the apical end of epithelial cells, are known to be concentrated in microvilli and at tight junctions, respectively. The intensity of moesin and ZO-1 staining in the contact regions of each cell was markedly higher in HepG2/SMP30 than in control cells. Moreover, moesin stained more interior areas, which corresponded to the microvilli of bile canaliculi. Clearly, bile canaliculi with microvilli formed at the apical ends of HepG2/SMP30 cells. These results indicate that SMP30 has an important physiological function as a participant in cell-to-cell interactions and imply that the downregulation of SMP30 during the aging process contributes to the deterioration of cellular interactivity.

Deficiency of SMP30

Originally, SMP30 was discovered because of its decrease with aging. If this decrease is long lasting, the deficiency of SMP30 in animal models can be regarded

as an ultimate decrease approaching zero. To elucidate the effect of this SMP30 decrease with aging, we introduced a null mutation of the *SMP30* gene into the germ line of mice.[25]

Despite the complete lack of SMP30, these mutant (SMP30-knockout) mice were indistinguishable from their wild-type littermates in terms of development and fertilization capability. We then investigated tissues' susceptibility for apoptosis induced by cytokines using primary cultured hepatocytes, because SMP30 could rescue cells from death caused by a calcium influx, using a calcium ionophore as previously described.[13,14] In SMP30-knockout mice, hepatocytes were more susceptible to apoptosis induced by tumor necrosis factor-α (TNF-α) plus actinomycin D (ActD) than hepatocytes from wild-type mice. In addition, the TNF-α/ActD-induced caspase-8 activity in hepatocytes from SMP30-knockout mice was twofold greater than that in matched cells from wild-type mice. In contrast, no significant difference was observed in the TNF-α/ActD-induced NFκB activation of hepatocytes from wild-type versus SMP30-knockout mice, indicating that SMP30 is not related to TNF-α/ActD-induced NFκB activation itself.

Moreover, deletion of the *SMP30* gene enhanced the susceptibility to another apoptosis inducer. After we treated SMP30-knockout mice with sub-lethal amounts of anti-Fas antibodies, liver injury was prominent in SMP30-knockout mice but not wild-type mice (Fig. 4).[25] Collectively, these results demonstrate that SMP30 acts to protect cells from apoptosis and other cell injuries.

Another molecular mechanism for the anti-apoptotic function of SMP30 was reported by our collaborators.[26] When cells were exposed to TNF-α plus ActD, cell viability was threefold higher in HepG2/SMP30 than control HepG2 cells. The presence of trifluoperazine, a calmodulin inhibitor, attenuated the anti-apoptotic effect of SMP30 in both cell types, but the effect was more prominent in HepG2/SMP30.

Western blot analyses revealed that Akt[27,28] as a survival factor was activated in HepG2/SMP30 cells in the presence or absence of TNF-α plus ActD. However, the activation was not observed in control HepG2 cells. Further, trifluoperazine inhibited Akt activation in HepG2/SMP30 cells. We therefore propose that interplay between calmodulin and SMP30 regulates Akt activity and, thus, that SMP30 acts as a survival factor in hepatocytes.

Next, we evaluated the effect of a SMP30 deficiency on life span.[29] SMP30-knockout mice are viable and fertile but lower in bodyweight and shorter in lifespan

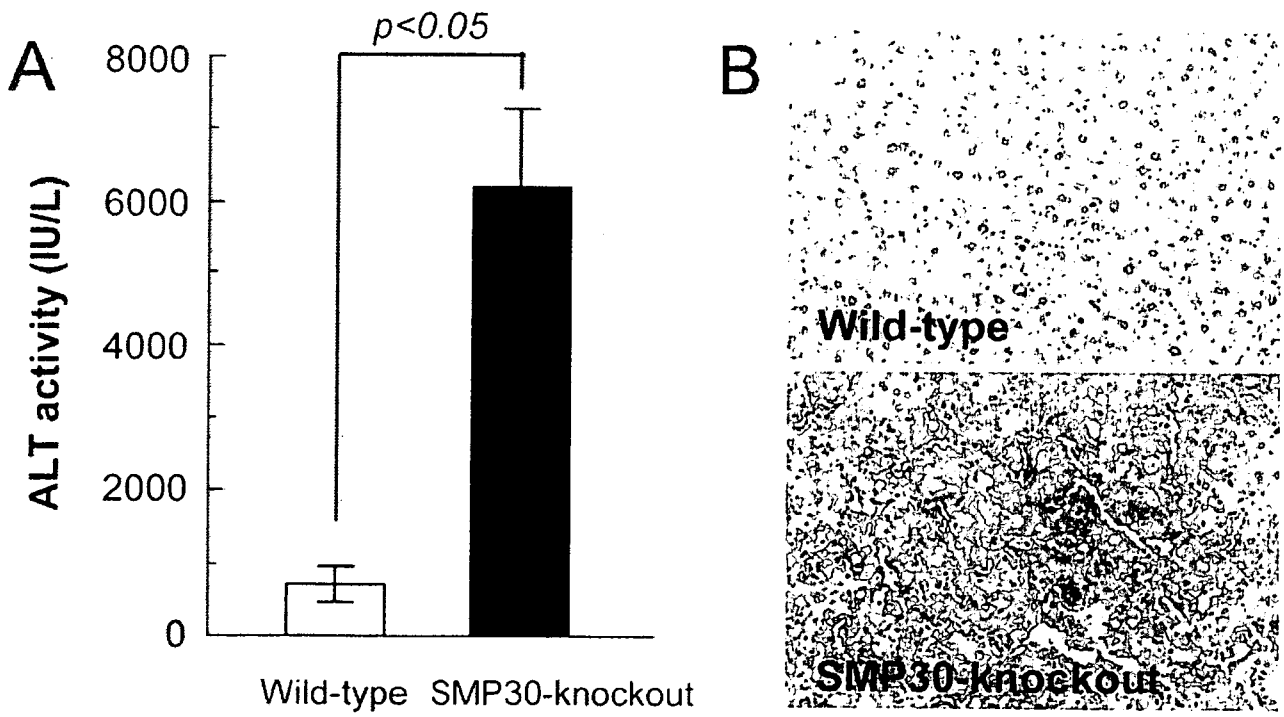

Figure 4 Anti-apoptotic activity of SMP30. Sub-lethal amounts of anti-Fas antibody were applied to SMP30-knockout and wild-type mice. (a) Serum alanine aminotransferase (ALT) levels of SMP30-knockout mice is higher than that of wild-type mice in peripheral blood after anti-Fas antibodies are applied. (b) Massive hemorrhage is visible in livers of SMP30-knockout mice but not wild-type mice.

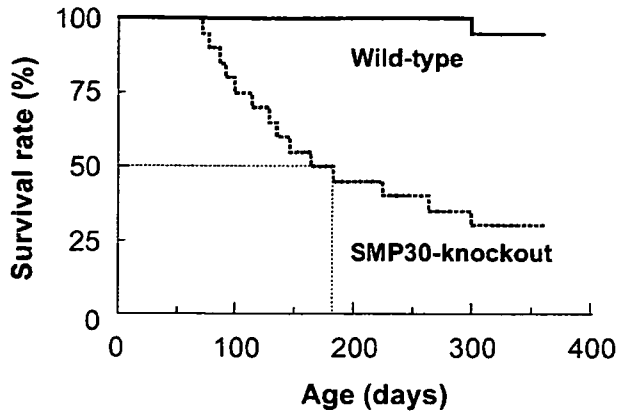

Figure 5 The lifespan is shortened in SMP30-knockout mice whose survival time was only 50%; that is, 180 days (6 months), in the 20 animals studied for comparison to the wild-type.

than their wild-type counterparts (Fig. 5). Histopathological examination showed no particular cause of the death in SMP30-knockout mice. The only noticeable event was marked emaciation in each individual. This finding suggests that the lack of SMP30 seems to be a model of "natural death." Because death often occurs in a background of malnutrition, the genuine cause deserves further study.

Via electron microscopy, hepatocytes from SMP30-knockout but not the wild-type mice at 12 months of age clearly contained many lipid droplets, abnormally enlarged mitochondria with indistinct cristae and enlarged lysosomes filled with electron-dense bodies. In liver specimens from SMP30-knockout mice, the marked number of lipid droplets visible around the central vein increased notably in size and amount as the animals aged. Biochemical analysis of neutral lipids, total hepatic triglycerides and cholesterol from SMP30-knockout mice showed approximately 3.6- and 3.3-fold higher levels, respectively, than those from age-matched wild-type mice. Moreover, values for total hepatic phospholipids from SMP30-knockout mice were approximately 3.7-fold higher than those for their wild-type counterparts.

By thin-layer chromatography analysis, phosphatidylethanolamine, cardiolipin, phosphatidylcholine, phosphatidylserine and sphingomyelin accumulations were detected in lipid extracts from the livers of SMP30-knockout mice. Conceivably, this abnormal lipid metabolism might be one cause of the shortened lifespan of these mice without SMP30.

Because SMP30 is expressed in almost all organs except those with hematopoietic function, we widened our search for the pathological features of aging beyond those in the liver and kidneys. As we previously reported, SMP30-knockout mice are novel models of senile lungs with age-related airspace enlargement and enhanced susceptibility to harmful stimuli.[30] Aging and smoking are considered as major contributing factors for the development of pulmonary emphysema. For that reason, we evaluated whether SMP30-knockout mice are susceptible to oxidative stress associated with aging and smoking.[31] In the lungs of SMP30-knockout mice, protein carbonyls tended to increase with aging and were significantly higher than in the age-matched wild-type mice. Exposure to cigarette smoke generated marked airspace enlargement with significant parenchymal destruction in the SMP30-knockout mice than in the wild-type mice. The protein carbonyls, malondialdehyde, total glutathione and apoptosis of lung cells were significantly increased after an 8-week exposure to cigarette smoke in the SMP30-knockout mice. Because our results suggest that SMP30 protects the lungs from oxidative stress associated with aging and smoking, the SMP30-knockout mouse could be a useful animal model for investigating age-related lung diseases such as emphysema.

In submandibular glands, the influence of a SMP30 deficiency is more intense than in other organs. For example, marked swelling of mitochondria and decreased numbers of secretory granules can be observed in 12-month old SMP30-knockout mice (Fig. 6).[32]

The expression of SMP30 in the brain has been detected, although at a very low level. Nevertheless, the effect of this deficiency is prominent.[33] We showed that the generation of reactive oxygen species (ROS) and nicotinamide adenine dinucleotide phosphate (NADPH) oxidase activities were significantly elevated in the brains of SMP30-knockout mice. The increased oxidative status in these mice was further confirmed by their increases of oxidatively modified proteins such as dityrosine formation and carbonylation in the cerebral cortex. Moreover, the brains of SMP30-knockout mice manifested increased amounts of Mac-1,[34] which is regarded as the key mediator responsible for the migration of neutrophil, protein and myeloperoxidase activity, supporting the putative anti-oxidative action of SMP30. Interestingly, the activities of other major anti-oxidant enzymes (i.e. superoxide dismutase, catalase and glutathione peroxidase) in the brain were not affected by SMP30 depletion. Our results documented that, in the brain, SMP30 has a protective action against oxidative damage without influencing anti-oxidant enzyme status.

Two morphological features considered to be a hallmark of senescence are apparent in SMP30-knockout mice. At 12-months of age, SMP30-knockout mice had clearly visible deposits of lipofuscin and senescent-associated β-galactosidase in their renal tubular epithelia.[35] These features are compatible with high electron dense deposits in lysosomes. This observation supports

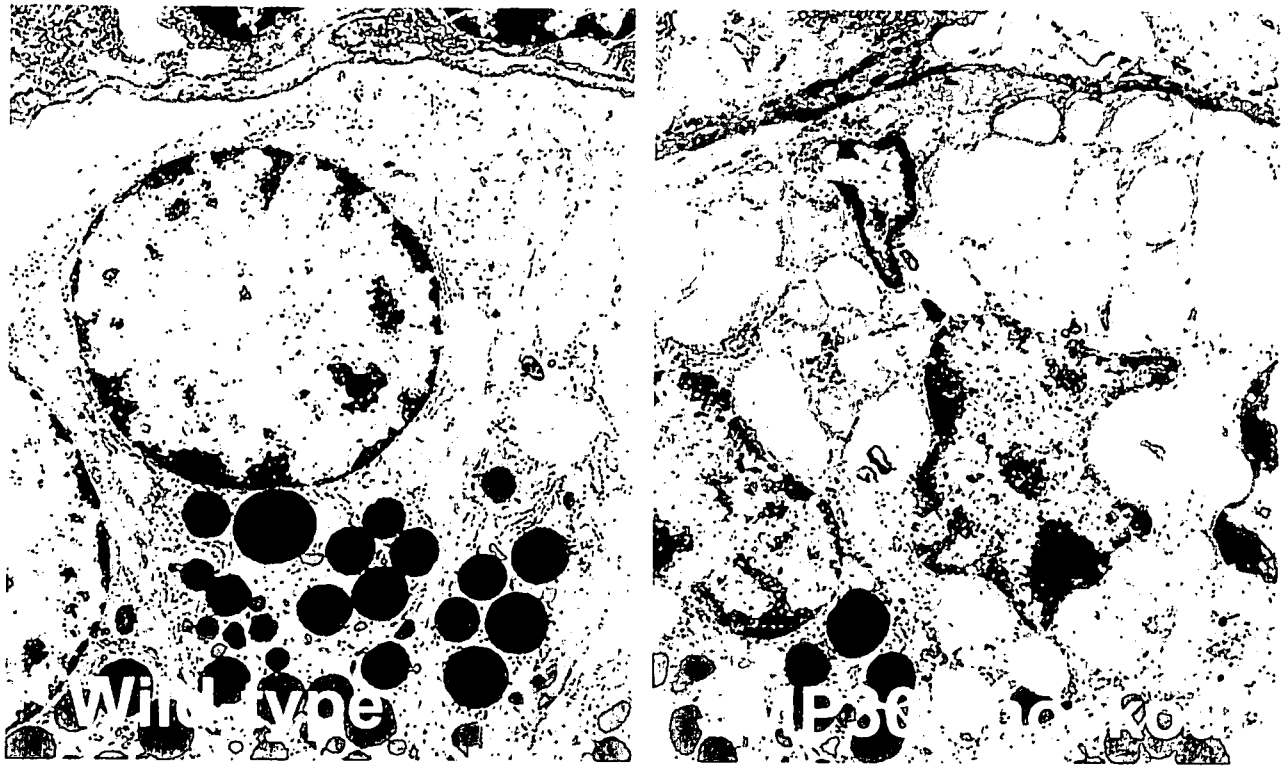

Figure 6 Degenerative subcellular components in SMP30-knockout mice. Granular duct cells of submandibular glands from a 37-week old SMP30-knockout mouse shows swollen mitochondria and a decrease of secretory granules.

the conclusion that the SMP30-knockout mouse is a useful model of ordinal senescence.

Most importantly, we have now identified an indisputable function of SMP30, that is, the production of vitamin C.[20] Because vitamin C is uniformly regarded as an anti-oxidant, we and others believe that a shortage of vitamin C induces senescence. This assumption has been proved by our observation that the lifespan of SMP30-knockout mice is significantly shorter than that of matched wild-type mice (Fig. 5).[29]

Modulation of SMP30

The suppressive effect of SMP30 on senescence has been introduced in this review. The other side of that coin is also true; enhancement of SMP30 expression prevents the pleiotropic dysfunction of organs during the aging process. Based on our studies, one can conclude that, in this context, the most influential factor causing senescence is oxidative stress. The relationship between SMP30 expression and oxidative stress is critical for understanding the mechanisms of senescence.

We used calorie restriction to explore age-related changes in *SMP30* gene expression.[36] The restriction of calories is the most probable paradigm for manipulating the development of senescence in humans.[37] The thrust of our investigation was based on the ability of calorie restriction to defend against age-related oxidative stress and the inflammatory process. The rats used for these experiments were divided into two groups: those fed ad libitum and those given a 40% calorie restricted diet. As expected, the animals' SMP30 expression declined with age, but in the calorie restricted group, this decline was clearly blunted (Fig. 7). Our data showed that the downregulation of SMP30 was accompanied by an increased generation of ROS, the oxygen-reactive entity. Therefore, the potent anti-aging and anti-oxidative action of a low-calorie diet effectively suppressed the age-related downregulation of SMP30 by ROS reduction.

Because age-related changes in SMP30 expression can be modulated by anti-oxidative action, the modulation of *SMP30* gene expression was explored by: (i) anti-oxidative calorie restriction of rats; (ii) pro-inflammatory lipopolysaccharide (LPS) administration to aged rats; (iii) oxidative stress promoter, *tert*-butylhydroperoxide (t-BHP) injection of mice; and (iv) t-BHP-treatment of Ac2F cells, a normal rat liver cell line.[38] We focused on the binding activity of an unidentified transcription factor at two sites located in the SMP30 promoter region.[39] Our results showed, first, that a calorie-restricted diet prevented the age-related decrease in SMP30 expression. Second, the binding of

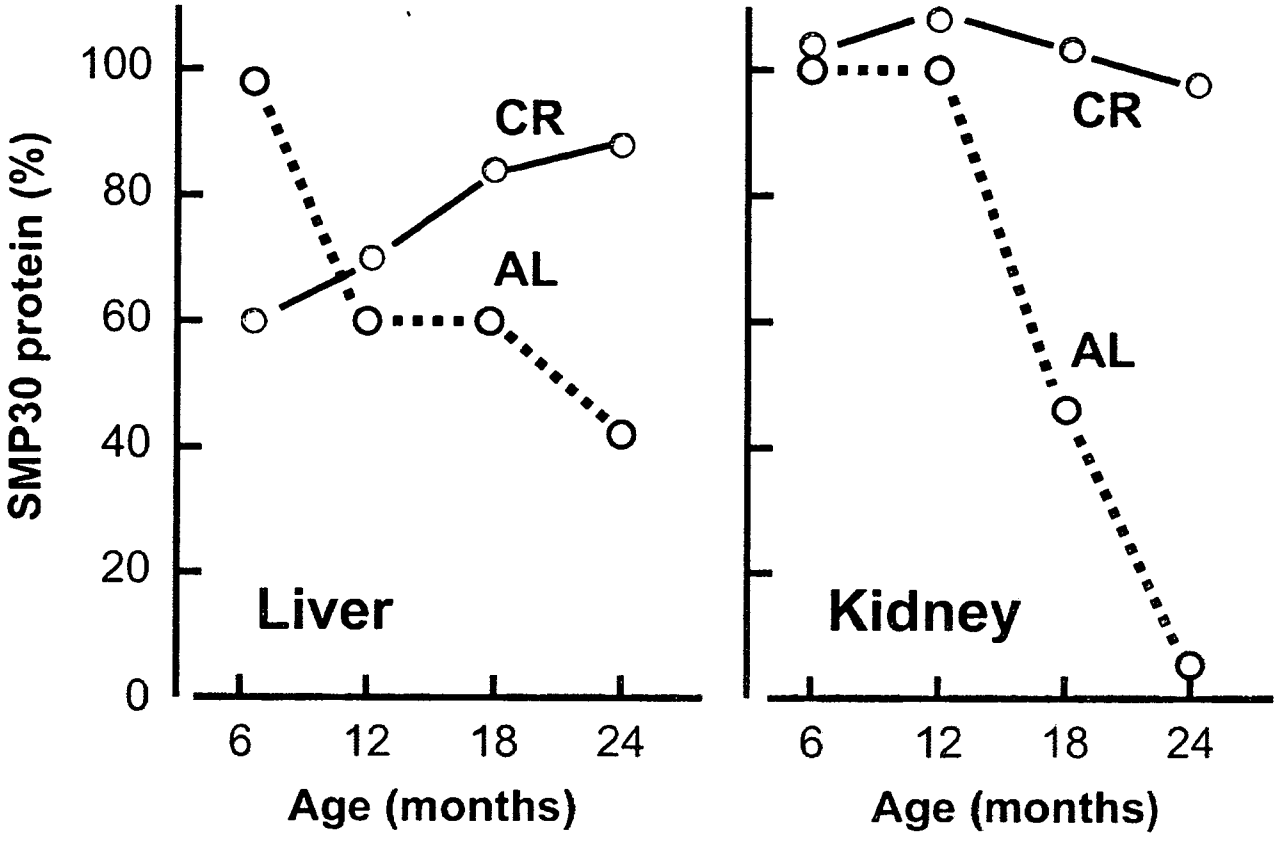

Figure 7 Enhanced SMP30 protein levels in the liver and kidneys from a calorie restricted (CR) diet. Rats were divided into an ad libitum fed group (AD) and a 40% CR group.

this transcription factor to the two sites in the SMP30 promoter region decreased after treatment with t-BHP or LPS. These findings were confirmed by using the anti-oxidant NAC and the ERK-specific inhibitor PD098059, both of which blunted the decrease in *SMP30* gene expression. Third, the binding by t-BHP also diminished at both sites in the Ac2F cell system. These outcomes strongly indicate that the SMP30 transcriptional process is redox-sensitive and that its modulation occurs at DNA binding sites in the promoter region. The downregulation of SMP30 likely involves the ERK signal pathway.

Conclusions

Proteomics analysis has provided us with a large amount of information about aging in general and, in particular, about age-associated molecules including SMP30. This factor is one of the best prospects for elucidating the mechanism of senescence, as we have done in functional analyses of multiple organs. We propose that the SMP30-knockout murine strain, in which SMP30 is completely absent, is the most useful model available for understanding human aging. In fact, the absence of SMP30 is the reason why this strain lacks an enzyme responsible for the synthesis of vitamin C as an anti-oxidant. Further research on the biological functions of SMP30 will assuredly produce useful tools for treating or offsetting the deleterious effects of aging in humans.

Acknowledgments

This work is supported by the NOVARTIS Foundation for Gerontological Research. A grant from the Japanese Ministry of Education, Culture, Sports, Science, and Technology and a grant from Health Science Research Grants for Comprehensive Research on Aging and Health supported by the Ministry of Health, Labor, and Welfare of Japan are acknowledged. The excellent assistance in the review of English by Ms P. Minick is gratefully acknowledged.

References

1 Tahara S, Kaneko T. Susceptibility of mouse splenic cells to oxidative DNA damage by x-ray irradiation. *Biol Pharm Bull* 2004; 27: 105–108.

2 Nawata H, Yanase T, Goto K, Okabe T, Ashida K. Mechanism of action of anti-aging DHEA-S and the replacement of DHEA-S. *Mech Ageing Dev* 2002; **123**: 1101–1106.
3 Hosokawa M. A higher oxidative status accelerates senescence and aggravates age-dependent disorders in SAMP strains of mice. *Mech Ageing Dev* 2002; **123**: 1553–1561.
4 Kuro-oM, Matsumura Y, Aizawa H *et al.* Mutation of the mouse klotho gene leads to a syndrome resembling ageing. *Nature* 1997; **390**: 45–51.
5 Fujita T, Uchida K, Maruyama N. Purification of senescence marker protein-30 (SMP30) and its androgen-independent decrease with age in the rat liver. *Biochim Biophys Acta* 1992; **1116**: 122–128.
6 Ishigami A, Handa S, Maruyama N, Supakar PC. Nuclear localization of senescence marker protein-30, SMP30, in cultured mouse hepatocytes and its similarity to RNA polymerase. *Biosci Biotechnol Biochem* 2003; **67**: 158–160.
7 Fujita T, Shirasawa T, Uchida K, Maruyama N. Isolation of cDNA clone encoding rat senescence marker protein-30 (SMP30) and its tissue distribution. *Biochim Biophys Acta* 1992; **1132**: 297–305.
8 Fujita T, Mandel JL, Shirasawa T, Hino O, Shirai T, Maruyama N. Isolation of cDNA clone encoding human homologue of senescence marker protein-30 (SMP30) and its location on the X chromosome. *Biochim Biophys Acta* 1995; **1263**: 249–252.
9 Fujita T, Shirasawa T, Maruyama N. Isolation and characterization of genomic and cDNA clones encoding mouse senescence marker protein-30 (SMP30). *Biochim Biophys Acta* 1996; **1308**: 49–57.
10 Goto SG. Expression of Drosophila homologue of senescence marker protein-30 during cold acclimation. *J Insect Physiol* 2000; **46**: 1111–1120.
11 Nakajima Y, Natori S. Identification and characterization of an anterior fat body protein in an insect. *J Biochem (Tokyo)* 2000; **127**: 901–908.
12 Kondo Y, Ishigami A, Kubo S *et al.* Senescence marker protein-30 is a unique enzyme that hydrolyzes diisopropyl phosphorofluoridate in the liver. *FEBS Lett* 2004; **570**: 57–62.
13 Fujita T, Inoue H, Kitamura T, Sato N, Shimosawa T, Maruyama N. Senescence marker protein-30 (SMP30) rescues cell death by enhancing plasma membrane Ca^{2+}-pumping activity in Hep G2 cells. *Biochem Biophys Res Commun* 1998; **250**: 374–380.
14 Inoue H, Fujita T, Kitamura T *et al.* Senescence marker protein-30 (SMP30) enhances the calcium efflux from renal tubular epithelial cells. *Clin Exp Nephr* 1999; **3**: 261–267.
15 Billecke SS, Primo-Parmo SL, Dunlop CS, Doorn JA, La Du BN, Broomfield CA. Characterization of a soluble mouse liver enzyme capable of hydrolyzing diisopropyl phosphorofluoridate. *Chem Biol Interact* 1999; **119–120**: 251–256.
16 Little JS, Broomfield CA, Fox-Talbot MK, Boucher LJ, MacIver B, Lenz DE. Partial characterization of an enzyme that hydrolyzes sarin, soman, tabun, and diisopropyl phosphorofluoridate (DFP). *Biochem Pharmacol* 1989; **38**: 23–29.
17 Gomi K, Kajiyama N. Oxyluciferin, a luminescence product of firefly luciferase, is enzymatically regenerated into luciferin. *J Biol Chem* 2001; **276**: 36508–36513.
18 Gomi K, Hirokawa K, Kajiyama N. Molecular cloning and expression of the cDNAs encoding luciferin-regenerating enzyme from Luciola cruciata and Luciola lateralis. *Gene* 2002; **294**: 157–166.
19 Kanagasundaram V, Scopes R. Isolation and characterization of the gene encoding gluconolactonase from Zymomonas mobilis. *Biochim Biophys Acta* 1992; **1171**: 198–200.
20 Kondo Y, Inai Y, Sato Y *et al.* Senescence marker protein 30 functions as gluconolactonase in l-ascorbic acid biosynthesis, and its knockout mice are prone to scurvy. *Proc Natl Acad Sci USA* 2006; **103**: 5723–5728.
21 Brodie AF, Lipmann F. Identification of a gluconolactonase. *J Biol Chem* 1955; **212**: 677–685.
22 Ishigami A, Fujita T, Inoue H *et al.* Senescence marker protein-30 (SMP30) induces formation of microvilli and bile canaliculi in Hep G2 cells. *Cell Tissue Res* 2005; **320**: 243–249.
23 Takeuchi K, Sato N, Kasahara H *et al.* Perturbation of cell adhesion and microvilli formation by antisense oligonucleotides to ERM family members. *J Cell Biol* 1994; **125**: 1371–1384.
24 Ando-Akatsuka Y, Yonemura S, Itoh M, Furuse M, Tsukita S. Differential behavior of E-cadherin and occludin in their colocalization with ZO-1 during the establishment of epithelial cell polarity. *J Cell Physiol* 1999; **179**: 115–125.
25 Ishigami A, Fujita T, Handa S *et al.* Senescence marker protein-30 knockout mouse liver is highly susceptible to tumor necrosis factor-α- and Fas-mediated apoptosis. *Am J Pathol* 2002; **161**: 1273–1281.
26 Matsuyama S, Kitamura T, Enomoto N *et al.* Senescence marker protein-30 regulates Akt activity and contributes to cell survival in Hep G2 cells. *Biochem Biophys Res Commun* 2004; **321**: 386–390.
27 Cheng A, Wang S, Yang D, Xiao R, Mattson MP. Calmodulin mediates brain-derived neurotrophic factor cell survival signaling upstream of Akt kinase in embryonic neocortical neurons. *J Biol Chem* 2003; **278**: 7591–7599.
28 Egea J, Espinet C, Soler RM *et al.* Neuronal survival induced by neurotrophins requires calmodulin. *J Cell Biol* 2001; **154**: 585–598.
29 Ishigami A, Kondo Y, Nanba R *et al.* SMP30 deficiency in mice causes an accumulation of neutral lipids and phospholipids in the liver and shortens the life span. *Biochem Biophys Res Commun* 2004; **315**: 575–580.
30 Mori T, Ishigami A, Seyama K *et al.* Senescence marker protein-30 knockout mouse as a novel murine model of senile lung. *Pathol Int* 2004; **54**: 167–173.
31 Sato T, Seyama K, Sato Y *et al.* Senescence marker protein-30 protects mice lungs from oxidative stress, aging, and smoking. *Am J Respir Crit Care Med* 2006; **174**: 530–537.
32 Ishii K, Tsubaki T, Fujita K, Ishigami A, Maruyama N, Akita M. Immunohistochemical localization of senescence marker protein-30 (SMP30) in the submandibular gland and ultrastructural changes of the granular duct cells in SMP30 knockout mice. *Histol Histopathol* 2005; **20**: 761–768.
33 Son TG, Zou Y, Jung KJ *et al.* SMP30 deficiency causes increased oxidative stress in brain. *Mech Ageing Dev* 2006; **127**: 451–457.
34 Clark RS, Carlos TM, Schiding JK. Antibodies against Mac-1 attenuate neutrophil accumulation after traumatic brain injury in rats. *J Neurotrauma* 1996; **13**: 333–341.
35 Yumura W, Imasawa T, Suganuma S *et al.* Accelerated tubular cell senescence in SMP30 knockout mice. *Histol Histopathol* 2006; **21**: 1151–1156.
36 Jung KJ, Ishigami A, Maruyama N *et al.* Modulation of gene expression of SMP-30 by LPS and calorie restriction during aging process. *Exp Gerontol* 2004; **39**: 1169–1177.

37 Lane MA, Baer DJ, Rumpler WV *et al.* Calorie restriction lowers body temperature in rhesus monkeys, consistent with a postulated anti-aging mechanism in rodents. *Proc Natl Acad Sci USA* 1996; **93**: 4159–4164.
38 Jung KJ, Maruyama N, Ishigami A, Yu BP, Chung HY. The redox-sensitive DNA binding sites responsible for age-related downregulation of SMP30 by ERK pathway and reversal by calorie restriction. *Antioxid Redox Signal* 2006; **8**: 671–680.
39 Supakar PC, Fujita T, Maruyama N. Identification of novel sequence-specific nuclear factors interacting with mouse senescence marker protein-30 gene promoter. *Biochem Biophys Res Commun* 2000; **272**: 436–440.

European Journal of Neurology 2007, 14: 1029–1034 doi:10.1111/j.1468-1331.2007.01870.x

Clinical and experimental features of MuSK antibody positive MG in Japan

K. Ohta[a], K. Shigemoto[b], A. Fujinami[c], N. Maruyama[d], T. Konishi[e] and M. Ohta[a,c]

[a]*Clinical Research Center, Utano National Hospital, Kyoto, Japan;* [b]*Department of Preventive Medicine, Faculty of Medicine, Graduate School of Ehime University, Ehime, Japan;* [c]*Department of Medical Biochemistry, Kobe Pharmaceutical University, Kobe, Japan;* [d]*Tokyo Metropolitan Institute of Gerontology, Tokyo, Japan; and* [e]*Department of Neurology, Utano National Hospital, Kyoto, Japan*

Keywords:
clinical features, domain, IgG subclass, muscle specific tyrosine kinase, MuSK antibody, myasthenia gravis, seronegative myasthenia gravis

Received 28 December 2006
Accepted 7 May 2007

We investigated the presence of antibodies (Abs) against muscle-specific tyrosine kinase (MuSK) in Japanese myasthenia gravis (MG) patients. MuSK Abs were found in 23 (27%) of 85 generalized seronegative MG (SNMG) patients but not in any of the ocular MG patients. MuSK Ab-positive patients were characterized as having female dominance (M:F, 5:18), age range at onset 18 to 72 (median 45) years old, and prominent oculobulbar symptoms (100%) with neck (57%) or respiratory (35%) muscle weakness. Limb muscle weakness was comparatively less severe (52%), thymoma absent. Most patients had good responses to simple plasma exchange and steroid therapy. MuSK IgG from all 18 patients was exclusively the IgG 4 subclass and bound mainly with the MuSK Ig 1–2 domain. Serial studies of 12 individuals showed a close correlation between the variation in MuSK Ab titers and MG clinical severity ($P = 0.01$ by Kruskal–Wallis). MuSK Ab titers were sharply decreased in patients who had a good response to early steroid therapy or simple plasma exchange, but there was no change, or a rapid increase on exacerbation after thymectomy. Measurement of MuSK Ab titers aids in the diagnosis of MG and the monitoring of clinical courses after treatment.

Introduction

Muscular weakness in most patients with myasthenia gravis (MG) is caused by an antibody (Ab)-mediated autoimmune response to muscle nicotinic acetylcholine receptors (AChRs), but there is no correlation between the AChR Ab level and degree of muscle weakness. This may be because of AChR Abs heterogeneity and epitope specificity or the presence of Abs against other functionally important muscle antigens. Fifteen percent of patients with generalized MG who have no detectable circulating Abs to AChR are termed seronegative MG (SNMG). Autoantibodies against muscle-specific tyrosine kinase (MuSK) have been identified in that population [1]. The positivity for MuSK Ab in SNMG patients varied from 3.8% to 71% by studies [1–11], which may be due to geographical or ethnic differences. Immunoglobulin allotypes in Caucasian and Chinese MG patients differ from those in Japanese patients [12]. We performed a MuSK Ab survey of a large number of Japanese MG patients and characterized the clinical features of those who were MuSK Ab positive. Furthermore, we investigated the correlation between MuSK Ab titer and disease severity, epitope specificity, and the IgG subclass of MuSK IgG.

Correspondence: Mitsuhiro Ohta, Department of Medical Biochemistry, Kobe Pharmaceutical University, Motoyamakita, Higashinada-ku, Kobe 658–8558, Japan (tel.: +81 78 441 7557; fax: +81 78 441 7559; e-mail: mohta@kobepharma-u.ac.jp).

Patients and methods

Patients

We studied 85 patients (27 men, 58 women, mean age 56 years old, range 18–76 years) who had generalized SNMG and were consistently negative for serum AChR Abs, as well as 272 AChR Ab-positive MG (SPMG) patients (87 men, 185 women, mean age 54 years old; age range 32–74 years); 50 with and 222 without thymoma. The control populations comprised 70 healthy participants (29 men, 41 women; mean age 50 years old, range 27–74 years) and 91 patients (37 men, 54 women; mean age 50 years old, range 32–74 years) with other neurological or immunological diseases (five Lambert-Eaton myasthenic syndrome, six polymyositis, 10 muscular dystrophy, 15 thyroiditis, 10 type 1 diabetes mellitus, five rheumatoid arthritis, 10 multiple sclerosis, five spinal progressive muscular atrophy, five chronic inflammatory demyelinating polyneuropathy, 10 amyotrophic lateral sclerosis, and 10 epilepsy). The study was approved by the ethics committee of Utano National Hospital. All persons gave their informed consent prior to their inclusion in the study.

Preparation of recombinant human MuSK protein

To produce his-tag human MuSK protein, the entire extracellular domain (MuSK 1–4; nucleotides 107–1526,

GenBank/EMBL accession number AF006464) of human MuSK, and MuSK fragments comprised of the first half bearing two Ig-domains (MuSK 1–2; nucleotides 107–700) were linked to the PCR3.1/Myc-His vector (Invitrogen Corporation, Carlsbad, CA, USA) [13]. Membrane-proximal extracellular domains, including Ig-domains 3 and 4 (MuSK 3–4; nucleotides 701–1526), were linked to the pSecTag-His vector (Invitrogen) carrying the ER signal sequence of the mouse Igκ gene. All constructs were transiently transfected to COS7 cells [14]. The recombinant his-tag MuSK secreted was purified in a histidine-affinity column (Clonetech Laboratories, Palo Alto, CA, USA). Recombinant protein purity was determined by SDS-PAGE with silver staining. Recombinant protein concentrations were obtained with a BCA Protein assay kit (Pierce, Biotechnology, Inc., Rockfold, IL, USA) with bovine serum albumin as the standard. The MuSK extracellular domain and MuSK fragments then were labeled with ^{125}I [15].

Detection of MuSK Ab by radioimmunoprecipitation assay

All the sera underwent a radioimmunoassay (RIA) to determine the presence of MuSK Ab. In brief, 5 μl of each sample was incubated overnight at 4°C with 50 μl of ^{125}I-his-tag MuSK (40 000 cpm), after which 50 μl of anti-human IgG was added, and the sample incubated for another 2 h at room temperature. Radioactivity was counted after two washes of the pellets with saline. All positive sera were titrated, and results expressed as nanomoles of ^{125}I-MuSK precipitated per liter of serum.

Epitope mapping

Muscle-specific tyrosine kinase Ab-positive sera were tested by an RIA for the presence of IgG Abs to MuSK 1–2 or MuSK 3–4. In brief, 5 μl of each sample was incubated overnight at 4°C with ^{125}I-his-tag MuSK (40 000 cpm), ^{125}I-his-tag MuSK 1–2 (30 000 cpm), or ^{125}I-his-tag MuSK 3–4 (30 000 cpm), after which 50 μl of anti-human IgG was added. The samples then were incubated for another 2 h at room temperature. Radioactivity was counted after two washes of the pellets with saline.

IgG subclasses of MuSK Ab

Microtiter plates (Breakapart plate, Nunk-Immuno Module, Roskilde, Denmark) were coated with 100 μl of 10 μg/ml of each Ab to IgG subclasses (sheep polyclonal anti-human IgG1, 2, 3 and 4; Binding Site, Birmingham, UK) diluted with 10 mM sodium carbonate-bicarbonate buffer, pH 9.3 and kept for 1 h at room temperature. Nonspecific binding sites were saturated with 200 μl PBS containing 5% skimmed milk and 10% Blockace (Dainippon Seiyaku, Osaka, Japan) for 2 h at room temperature. A serum sample (20 μl), first incubated for 2 h at room temperature with ^{125}I-MuSK (30 000 cpm), was added to a plate, and the whole incubated for 2 h at room temperature. After four washes, ^{125}I was counted in each well.

Statistical analysis

Statistical analysis was performed by regression analysis, Kruskal–Wallis, one-way analysis of variance, and Student *t* test. A *P*-value of <0.05 was considered significant.

Results

MuSK Abs

The cut-off value (0.01 nM) was calculated from the mean + 3SD of the healthy subjects' values obtained by an RIA constructed with ^{125}I-MuSK extracellular domains. MuSK Ab was present in 23 (27%) of the 85 SNMG patients but not in any of the 272 SPMG patients, healthy subjects and patients with other neurological or immunological diseases (Fig. 1). Ab-positive samples were confirmed by serial dilution tests, and titers shown as nanomoles of ^{125}I-MuSK precipitated per liter of serum. MuSK Ab titers ranged from 8.4 to 240 nM (median, 57 nM). All the positive serum samples had extremely high titers on ^{125}I-human MuSK immunoprecipitation.

Clinical features of patients with MuSK Abs

Table 1 shows the clinical features of 23 MuSK Ab-positive patients. MuSK Ab in generalized SNMG showed female predominance (five men, 18 women) but not in ocular MG. Age at onset ranged from 18 to 72 years old (median 45 years). Clinical features of MuSK Ab-positive patients were confined to ocular [ptosis, 13/23 (57%) and double vision, 18/23 (78%)]; bulbar [dysphagia: 23/23 (100%), dysarthria: 19/23 (83%)]; neck extensor, 13/23 (57%); respiratory 8/23 (35%) muscle weaknesses. Prevailing weaknesses affected the oculobulbar and respiratory muscles of MuSK Ab-positive patients. About 48% (11/23) had no limb weakness. No thymomas were detected by CT. Six (26%) of the 23 MuSK Ab-positive patients who were thymectomized, had histological abnormalities including small hyperplastic features.

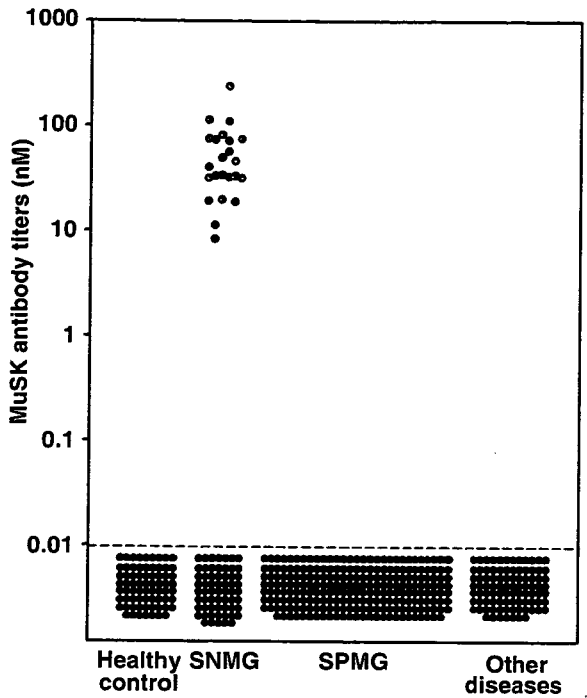

Figure 1 RIA-detected MuSK Ab titers of 85 patients with SNMG, 272 patients with SPMG, 91 patients with other neurological or immunological diseases, and 70 healthy participants. Broken line, the cutoff (0.01 nM) for MuSK Abs.

Table 1 Clinical features of MuSK Ab-positive patients

MuSK Ab positivity in SNMG	23/85 (27%)
MuSK Ab titers	8.4–239 (median 57 nM)
F:M	18:5
Age at onset	18–72 years (median 45 years)
Distribution of weakness	
Ptosis	13/23 (57%)
Ocular motor dysfunction	18/23 (78%)
Bulbar	23/23 (100%)
Neck	13/23 (57%)
Respiratory (crises)	8/23 (35%)
Limb	12/23 (52%)
Thymus	
Thymoma	0/23 (0%)
Hyperplasia	6/23 (26%)

Serial studies of clinical status and MuSK Abs

We measured MuSK Ab titer serially during the disease's course. Table 2 shows anti-MuSK Ab titers in relation to disease severity and duration, and immunosuppressive treatment (A), plasma exchange (B), or thymectomy (C). Disease severity was graded according to the Myasthenia Gravis Foundation of America (MGFA) classification [16] at the onset of myasthenic symptoms, in the maximally deteriorated state, and at

Table 2 Changes in MuSK Ab titers and in clinical status in MuSK Ab-positive patients

Case	Gender	Age at onset (years)	Duration (days)	MuSK Ab (nM)	MGFA classification	treatment
(A) Early steroid therapy						
P-1	F	18	0	39.3	IIIb	
			56	39.0		Pred
			82	40.2		Pred
			138	38.0		Pred
			175	35.0	IIb	Pred
			313	33.0	PR	Pred
			577	21.0		Pred
P-2	F	32	0	113.0	IVb	Pred
			141	17.0		Pred
			261	15.0	IIb	Pred
			409	16.0		Pred
P-3	F	48	0	80.0	IVb	Pred
			46	28.0		Pred
			101	5.0		Pred
			1,641	4.2	PR	Pred
P-4	F	53	0	36.8	IIIb	
			41	31.0		Pred
			97	15.2		Pred
			111	10.0	IIb	Pred
P-5	F	52	0	240.0	V	Pred
			49	57.0		Pred
			77	22.9		Pred
			101	8.4		Pred
			129	3.0	IIb	Pred
P-6	F	76	0	33.0	IIb	Pred
			83	0.5		Pred
			118	0.2	PR	Pred
(B) Simple plasma exchange (PE)						
P-7	M	53	0	74.4	V	
			42	59.0		
			52	47.0		
			PE ——→			
			62	28.5	IIb	
			PE ——→			
			67	17.2		
			125	16.0		Pred
			132	11.5		Pred
			138	9.0	IIb	Pred
P-8	M	71	0	113.9	IVb	
			PE ——→			
			11	32.1		
			45	32.0		Pred
			219	31.0		Pred
			616	28.0	IIb	Pred
P-9	F	66	0	30.0	IIIb	
			45	40.5		
			361	32.0		
			PE ——→			
			374	14.0	IIb	
			379	21.2		
			389	29.9		
			403	35.5	IIIb	Pred, Cyclo
			441	25.0		Pred, Cyclo
			476	20.5	IIb	Pred, Cyclo

Table 2 (Continued)

(C) Thymectomy (Tx)						
P-10	F	47	0	20.0		
			47	26.0	IIb	
			Tx ——→			
			95	47.2	IIIb	Pred
			270	19.8	IIb	Pred
P-11	F	52	0	22.6	IIb	
			58	23.2		
			Tx ——→			
			170	21.1		Pred
			255	25.0	IIb	
P-12	F	48	0	16.5	IIb	
			95	17.6		
			Tx ——→			
			210	15.7		Pred
			274	17.0	IIb	

PR, Pharmacological Remission; Pred, Predonisolone; Cyclo, Cyclosporine.

the last clinic visit after or during treatment. As shown in Table 2a, six patients (P1–P6) who underwent early steroid therapy showed impressive clinical improvement associated with a sharp decrease in anti-MuSK Ab titer; from 39.3 to 21.0 nM (P-1), 113.0 to 16.0 nM (P-2), 80.0 to 4.2 nM (P-3), 36.8 to 10.0 nM (P-4), 240.0 to 3.0 nM (P-5), and 33.0 to 0.2 nM (P-6). MG severities showed clinical improvement from class IIIb to pharmacological remission (PR) (P-1), class IVb to IIb (P-2), class IVb to PR (P-3), class IIIb to IIb (P-4), class V to IIb (P-5), and class IIb to PR (P-6).

Muscle-specific tyrosine kinase Ab titers of three patients were measured in serial samples taken before and after simple plasma exchange (Table 2b). The patients responded dramatically to that therapy, Ab titers decreasing from 74.4 to 9.0 nM (P-7), 113.9 to 28.0 nM (P-8), and from 30.0 to 20.5 nM (P-9), indicative of clinical improvement from class V to IIb (P-7), class IVb to IIb (P-8), and class IIIb to IIb (P-9). Moreover, conventional immunosuppression maintained the clinical improvement initially achieved by plasma exchange. In one patient (P-9), the effect had tapered off 45 days after plasma exchange, and Ab titer and disease severity returned to the level before treatment. Prednisolone and cyclosporin administered after MG relapse resulted in slower improvement.

Three patients who had histological abnormalities, including a small hyperplastic thymus, underwent thymectomies (Table 2c). After surgery one patient (P-10) immediately had worsening of dysphagia from class IIb to IIIb associated with a rapid increase in MuSK Ab titer from 26.0 to 47.2 nM. Thymectomy was not effective for the other two patients (P-11, P-12) who showed no change in disease severity and MuSK Ab titer.

We analyzed MuSK Ab titers in relation to quantitative clinical scores on the MGFA scale in serial studies of 12 individuals. MuSK Ab titers and disease severity were correlated ($P = 0.01$ by Kruskal–Wallis).

Epitopes in the extracellular domains of human MuSK

Eighteen sera with MuSK Abs were examined for ^{125}I-MuSK 1–2 and ^{125}I-MuSK 3–4 binding. All predominantly bound to ^{125}I-MuSK 1–2, range 68–97%. Only five of the 18 sera also showed slight binding (20–30%) to ^{125}I-MuSK 3–4 (Table 3).

IgG subclasses of MuSK Abs

In a solid phase RIA with sheep polyclonal antibodies to human IgG subclasses, in all the 18 sera tested MuSK Abs were exclusively IgG4 (Table 4).

Discussion

The MuSK Ab-positive rate found for generalized SNMG patients in Japan was 27% with female predominance (M:F = 5:18). This rate is lower than the 70% positivity originally reported [1] and the 40–50% recently reported [2–7]. It is consistent with the 27–33% reported for Japanese and Korean population [8–10] but significantly higher than the 3.8% Chinese positivity rate [11]. Age at onset ranged from 18 to 72 years old (median, 45 years); 61% of the patients presenting at >40 years of age, later than for Caucasians, and 57–71% of patients presenting at <40 years of age, but the differences was not significant [3,7,17,18].

Table 3 Ratio of MuSK Ig 1–2 and 3–4 Ab in MuSK 1–4 Ab titers

Case	MuSK Ab (nM)	Ig 1–2 domain (%)	Ig 3–4 domain(%)
1	8.4	97.1	2.9
2	19.3	68.1	31.9
3	32.5	81.2	18.8
4	50.0	82.7	17.3
5	33.4	97.3	2.7
6	31.8	95.7	4.3
7	19.9	91.0	9.0
8	11.4	95.2	4.8
9	40.7	87.9	12.1
10	32.0	91.0	9.0
11	33.6	95.0	5.0
12	74.7	95.4	4.6
13	72.0	76.2	23.8
14	46.2	80.8	19.2
15	74.7	96.9	3.1
16	82.2	74.2	25.8
17	110.7	89.5	10.5
18	114.6	71.2	28.8

Table 4 Ratio of IgG subclasses of MuSK Abs

Case	MuSK Ab (nM)	IgG 1 (%)	IgG 2 (%)	IgG 3 (%)	IgG 4 (%)
1	114.6	0.0	0.0	0.0	100.0
2	110.7	0.0	0.0	4.9	95.1
3	82.2	0.0	0.0	0.0	100.0
4	74.7	11.0	21.0	19.0	49.0
5	74.0	4.1	5.0	5.6	85.3
6	72.0	0.0	1.0	0.0	99.0
7	46.2	0.0	0.0	0.0	100.0
8	40.7	5.3	0.0	7.1	87.6
9	33.6	15.1	15.7	0.0	69.2
10	33.4	0.0	0.0	0.0	100.0
11	32.5	5.3	0.0	0.0	94.7
12	32.0	4.2	2.6	1.2	92.0
13	31.8	6.7	6.7	8.3	78.3
14	19.9	0.0	0.0	1.7	98.3
15	19.5	0.0	0.0	0.0	100.0
16	19.3	0.0	0.0	0.0	100.0
17	11.4	0.0	28.9	26.1	45.0
18	8.4	0.0	0.0	0.0	100.0

All the Ab-positive patients had similar patterns of muscle weakness, with prevalent involvement of the bulbar muscles in 100%, ocular symptoms (blepharoptosis and/or double vision) in 80%, and of the respiratory muscles in 35% with frequent myasthenic crises. Limb muscle involvement was comparatively less severe and inconsistent. Japanese MuSK Ab-positive patients therefore have clinical features similar in terms of the predominance of bulbar involvement to those reported for Caucasians.

We evaluated the correlation between MuSK Ab titers and disease severity. Table 2 shows patients who had a good response to early immunosuppressive therapy or simple plasma exchange. Their MuSK Ab titers sharply decreased in parallel with clinical improvement, whereas their Ab titers remained positive. We evaluated the effect of thymectomy in three individuals by measuring MuSK Ab titers in serum samples taken pre- and post-thymectomy. One patient's condition deteriorated after thymectomy and her Ab titer greatly increased. The two others showed neither progression nor Ab titer change during the observation period. Thymectomy therefore did not produce good results. Histological changes in the thymus of MuSK Ab-positive subjects are reported to be minimal and to include rare small germinal centers [19,20] in contrast to SPMG patients who had lymph node-type infiltrates. These findings, together with the lack of benefit of thymectomy, are evidence against a role for the thymus in antigen presentation and antibody production.

Serial studies showed a statistically close correlation between MuSK Ab titers and disease severity. MuSK Ab titers also recently were found to correlate with MG severity [21]. MuSK Ab titers were extremely high in all the positive cases (Fig. 1). The close relationship between clinical status and MuSK Ab, found by monitoring Ab titers, suggests that MuSK Ab has a significant pathogenic role in MG patients. Circulating MuSK Abs, however, are reported not to cause a MuSK or AChR deficiency at the endplates [22]. Recent experimental models (rabbits [13] and mice [23]), developed by immunization with recombinant MuSK ectodomain protein, produced MG-like muscle weakness with reduced AChR clustering at neuromuscular junctions. These findings clarified the pathogenic MG mechanisms produced by MuSK Ab.

The paramount MuSK Ab IgG subclass in our eighteen patients was IgG4. Limb and intercostal muscle biopsies found neither reduction in AChR numbers nor complement deposition [9,24]. The absence of complement deposits at a patient's end plates is explained by the fact that MuSK Ab is mainly IgG class 4 which does not fix complement [5,25]. The MuSK extracellular domain consists of four MuSK immunoglobulin-like (Ig) domains. Binding analysis of MuSK Abs to ^{125}I-MuSK Ig 1–2 or ^{125}I-MuSK Ig 3–4 showed that the eighteen sera tested predominantly bound to the ^{125}I-MuSK Ig 1–2 domain. The epitope was the N-terminal of the extracellular domain of human MuSK as described previously [5]. Furthermore, MuSK Abs have been shown to inhibit agrin-induced clustering of AChRs [26]. In fact, MuSK Ig 1–2 domains are more responsible for agrin responsiveness of MuSK, in contrast to Ig 3-4 domains which are more responsible for rapsyn association. We postulate that this is relevant to our findings of predominant binding analysis to MuSK Ig 1–2. The characteristics of the MuSK IgG subclass and Ab binding epitope in Japanese patients therefore are similar to those of Caucasians.

Muscle-specific tyrosine kinase Ab-positive patients often suffer facial and tongue muscle atrophy [3,27]. Benveniste *et al.*[28] reported that MuSK Ab plasma may affect the expression of atrophy-related protein and that a facial muscle, the masseter, is the most susceptible. Amongst our MuSK Ab-positive patients, four patients had detectable tongue atrophy from a relatively early phase of illness; weakness was moderate in 2 patients and mild in two patients. More *in vitro* and *in vivo* studies are needed to clarify the pathologic mechanisms that cause the muscle weakness produced by MuSK Ab. MuSK Ab detection provides a valuable biological means of support for the clinical diagnosis of MG and a way to monitor its clinical course.

Acknowledgements

This study was supported in part by a grant-in-aid from the Ministry of Education, Culture, Sports, Science and

Technology, Japan, and grants from the High-Tech Research Center, the Kobe Pharmaceutical University Collaboration Fund, and the Science Research Promotion Fund of the Japan Private School Promotion Foundation.

References

1. Hoch W, McConville J, Helms S, Newsom-Davis J, Melms A, Vincent A. Auto-antibodies to the receptor tyrosine kinase MuSK in patients with myasthenia gravis without acetylcholine receptor antibodies. *Nature Medicine* 2001; **7:** 365–368.
2. Vincent A, Bowen J, Newsom-Davis J, McConville J. Seronegative generalized myasthenia gravis: clinical features, antibodies, and their targets. *Lancet Neurology* 2003; **2:** 99–106.
3. Evoli A, Tonali PA, Padua L, *et al.* Clinical correlates with anti-MuSK antibodies in generalized seronegative myasthenia gravis. *Brain* 2003; **126:** 2304–2311.
4. Sanders DB, EI-Salem K, Massey, JM, McConville J, Vincent A. Clinical aspects of MuSK antibody positive-seronegative MG. *Neurology* 2003; **60:** 1978–1980.
5. McConville J, Farrugia ME, Beeson D, *et al.* Detection and characterization of MuSK antibodies in seronegative Myasthenia gravis. *Annals of Neurology* 2004; **55:** 580–584.
6. Zhou L, McConville J, Chaudhry V, *et al.* Clinical comparison of muscle-specific tyrosine kinase (MuSK) antibody-positive and - negative myasthenic patients. *Muscle and Nerve* 2004; **30:** 55–60.
7. Padua L, Tonali P, Aprile I, *et al.* Seronegative myasthenia gravis: comparison of neurophysiological picture in MuSK+ and MuSK- patients. *European Journal of Neurology* 2006; **13:** 273–276.
8. Ohta K, Shigemoto K, Kubo S, *et al.* MuSK Ab described in seropositive MG sera found to be Ab to alkaline phosphatase. *Neurology* 2005; **65:** 1988.
9. Shiraishi H, Yoshimura T, Fukudome T, *et al.* Acetylcholine receptors loss and postsynaptic damage in MuSK antibody-positive myasthenia gravis. *Annals of Neurology* 2005; **57:** 289–293.
10. Lee JY, Sung JJ, Cho JY, *et al.* MuSK antibody-positive, seronegative myasthenia gravis in Korea. *Journal of Clinical Neuroscience* 2006; **13:** 353–355.
11. Yeh JH, Chen WH, Chiu HC, Vincent A. Low frequency of MuSK antibody in generalized seronegative myasthenia gravis among Chinese. *Neurology* 2004; **62:** 2131.
12. Chiu HC, de Lange GG, Willcox N, *et al.* Immunoglobulin allotypes in Caucasian and Chinese myasthenia gravis: differences from Japanese patients. *Journal of Neurology, Neurosurgery, and Psychiatry* 1988; **51:** 214–217.
13. Shigemoto K, Kubo S; Maruyama N, *et al.* Induction of myasthenia by immunization against muscle-specific kinase. *Journal of Clinical Investigation* 2006; **116:** 1016–1024.
14. Hopf C, Hoch W. Tyrosine phosphorylation of the muscle-specific kinase is exclusively induced by acetylcholine receptor-aggregation agrin fragments. *European Journal of Biochemistry* 1998; **253:** 382–389.
15. Hunter WM, Greenwood FC. Preparation of iodine-131 labeled human growth hormone of high specific activity. *Nature* 1962; **194:** 495–496.
16. Jaretzki A, Barohn RJ, Ernstoff RM, Kaminski HJ, Keesey JC, Penn AS. Myasthenia gravis: recommendations for clinical research standards. Task Force of the Medical Scientific Advisory Board of the Myasthenia Gravis Foundation of America. *Neurology* 2000; **55:** 16–23.
17. Lavrnic D, Losen M, Vujic A, *et al.* The features of myasthenia gravis with autoantibodies to MuSK. *Journal of Neurology, Neurosurgery, and Psychiatry* 2005; **76:** 1099–1102.
18. Diaz-Manera JA, Juarez C. Rojas-Garcia R, *et al.* Seronegative myasthenia gravis and antiMuSK positive antibodies: description of Spanish series. *Medicina Clinica (Barc)* 2005; **125:** 100–102.
19. Lauriola L, Ranelletti F, Maggiano N, *et al.* Thymus changes in anti-MuSK-positive and –negative myasthenia gravis. *Neurology* 2005; **64:** 536–538.
20. Leite MI, Strobel P, Jones M, *et al.* Fewer thymic changes in MuSK antibody-positive than in Musk antibody-negative MG. *Annals of Neurology* 2005; **57:** 444–448.
21. Bartoccioni E, Scuderi F, Minicuci GM, *et al.* Anti-Musk antibodies: correlation with myasthenia gravis severity. *Neurology* 2006; **67:** 505–507.
22. Selcen D, Fukuda T, Shen XM, Engel AG. Are MuSK antibodies the primary cause of myasthenic symptoms? *Neurology* 2004; **62:** 1945–1950.
23. Jha S, Xu K, Maruta T, *et al.* Myasthenia gravis induced in mice by immunization with the recombinant extracellular domain of rat muscle-specific kinase (MuSK). *Journal of Neuroimmunology* 2006; **175:** 107–117.
24. Vincent A, Leite MI. Neuromuscular junction autoimmune disease: muscle-specific kinase antibodies and treatments for myasthenia gravis. *Current Opinion in Neurology* 2005; **18:** 519–525.
25. Vincent A, Bowen J, Newsom-Davis J, McConville J. Seronegative generalized myasthenia gravis: clinical features and their targets. *Lancet Neurology* 2003; **2:** 99–106.
26. Farrugia ME, Bonifati DM, Clover L, Cossins J, Beeson D, Vincent A. Effect of sera from AChR-antibody negative myasthenia gravis patients on AChR and MuSK in cell cultures. *Journal of Neuroimmunology*, 2007; **185:** 136–144.
27. Farrugia ME, Robson MD, Clover L, *et al.* MRI and clinical studies of facial and bulbar muscle involvement in MuSK antibody-associated myasthenia gravis. *Brain* 2006; **129:** 1481–1492.
28. Benveniste O, Jacobson L, Farrugia ME, Clover L, Vincent A. MuSK antibody-positive myasthenia gravis plasma modifies MURF-1 expression in C2C12 cultures and mouse muscle in vivo. *Journal of Neuroimmunology* 2005; **170:** 41–48.

Acta Oto-Laryngologica, 2007; 127: 1024–1030

informa
healthcare

ORIGINAL ARTICLE

Quantitative analysis of mRNA in human temporal bones

YURIKA KIMURA[1,2,3], SACHIHO KUBO[2], HIROKO KODA[3], YOSHIHIRO NOGUCHI[3], MOTOJI SAWABE[4], NAOKI MARUYAMA[2] & KEN KITAMURA[3]

[1]*Departments of Otolaryngology and* [4]*Pathology, Tokyo Metropolitan Geriatric Hospital,* [2]*Aging Regulation Group, Research Team for Molecular Biomarkers, Tokyo Metropolitan Institute of Gerontolog and* [3]*Department of Otolaryngology, Graduate School, Tokyo Medical and Dental University, Tokyo, Japan*

Abstract

Conclusion. Well-preserved mRNA could be extracted from frozen human inner ears. Therefore, this study demonstrates that analysis of mRNA could be performed to study the molecular mechanisms of inner ear disorders using human specimens. *Objectives.* Analysis of RNA as well DNA is requisite to study the molecular mechanisms of inner ear disorders. Methods of isolating RNA from experimental animals have been established, while isolation of RNA from human inner ears is much more challenging. In the present study, we demonstrate a method by which messenger RNA (mRNA) was extracted from human inner ears and quantitatively analyzed. *Materials and methods. COCH* mRNA as well as *GAPDH* mRNA was extracted from membranous labyrinths dissected from three formalin-fixed and three frozen human temporal bones, removed at autopsy. The length of *COCH* mRNA and quantity of *GAPDH* mRNA was compared between the two groups by quantitative RT-PCR. *Results. COCH* mRNA could be amplified as much as 976 bp in all three frozen specimens. By contrast, it was amplified to 249 bp in two of the three formalin-fixed specimens, with no amplification observed in the remaining. The quantity of amplifiable *GAPDH* mRNA in the formalin specimens was only 1% of that of the frozen specimens.

Keywords: *Hearing loss, human, inner ear, mRNA, PCR*

Introduction

The mechanisms of sensorineural hearing loss have been analyzed with the recent advent of advanced molecular techniques. Studies of animals including mice have also contributed to identifying deafness genes and determining genotype–phenotype correlations [1,2]. In contrast, molecular analysis using human inner ear specimens is difficult because human inner ear specimens are inaccessible and formalin-fixed, celloidin-embedded temporal bone specimens are unsuitable for molecular analysis even though this method has been standard in histopathologic studies of the human temporal bones [3]. Nonetheless, there have been several reports in which DNA has been extracted from human inner ear specimens. Wackym et al. reported the first study using molecular biological techniques for human temporal bone pathology in 1993 [4]. They succeeded in amplifying mitochondria DNA by PCR and emphasized the difficulty of analyzing DNA from the human temporal bone because of the autolysis that occurs before fixation. They also reported PCR amplification of varicella-zoster virus DNA from temporal bone sections [5], as well as histopathologic analysis of a patient with Ramsay Hunt syndrome [6]. Moreover, the possibility of a relationship between presbycusis and a 4977 bp mtDNA deletion was suggested by PCR amplification of mtDNA from the cochlea of a celloidin-embedded human archival temporal bone [7]. We recently reported a quantitative analysis of mtDNA from a patient with a mutation at nucleotide 3243 [8] and detection of mitochondrial DNA from human inner ears using real-time PCR and laser microdissection [9] to elucidate mitochondrial hearing impairment. However, the availability of DNA analysis at a tissue level is limited to measurement of

Correspondence: Dr Ken Kitamura, Department of Otolaryngology, Tokyo Medical and Dental University, Graduate School, Yushima, Bunkyo-ku, Tokyo, 113-8519 Japan. Tel: +81 3 5803 5303. Fax: +81 3 5803 0146. E-mail: kitamura.oto@tmd.ac.jp

(Received 29 September 2006; accepted 14 December 2006)

ISSN 0001-6489 print/ISSN 1651-2551 online
DOI: 10.1080/00016480701200202

the heteroplasmy mutation ratio in mitochondrial hearing impairment or detection of a DNA virus, as mentioned above.

By contrast, analysis of mRNA expression patterns can demonstrate the spatio-temporal activities of gene transcription and expression in tissues, providing important physiological and pathological information at the molecular level [10]. Further, mRNA is important because it is a 'working copy' of a gene that directs biological activities of cells through the synthesis of proteins. Therefore, studying mRNA extracted from human inner ears can provide further information concerning the molecular mechanisms of inner ear disorders in humans. As removing temporal bones at autopsy is a regular method for studying human specimens, we analyzed and compared mRNA in formalin-fixed and frozen temporal bones removed at autopsy. The purpose of the present report was to establish the optimal method of extracting mRNA suitable for molecular biological applications from autopsied human temporal bones.

Materials and methods

Temporal bones

Six human temporal bones from five subjects with no hearing impairment (according to nursing records) were obtained at brain autopsy. Three were formalin-fixed and the others were put into the deep freezer as soon as possible after harvest and conserved by freezing at −80°C. The average age of the subjects was 77.0 years (range 72–83 years). The average time period between death and the start of autopsy was 20.1 h (range 4–47 h). Consent for using organs removed at autopsy was obtained from the patients' relatives. The present study was approved by the Ethical Review Board at Tokyo Metropolitan Geriatric Medical Hospital, pursuant to Article 18 of the Cadaver Autopsy and Preservation Act. Temporal bones were processed according to the surface preparation method (Figure 1) [11]. To avoid the degradation of RNA, we used RNAlater® (Ambion, Austin, TX, USA) to impregnate the temporal bone during the process and injected it into the inner ear from the oval window. The geniculate ganglion of facial nerves and the membranous labyrinth were dissected and immersed in a 1.5 ml microtube with 0.2 ml ISOGEN® (Nippon Gene, Tokyo, Japan).

Total RNA extraction and reverse transcription

Temporal bone samples were stored for an average of 7.5 months (range 2–18 months) before dissection. Dissected tissues were homogenized and mixed with 0.6 ml of ISOGEN®. After storage at room temperature for 5 min, 0.2 ml of chloroform was added. The mixture was shaken vigorously for 30 s, stored for 5 min at 4°C, and centrifuged at 15 000 g for 15 min at 4°C. The aqueous phase was transferred to microtubes, and 0.5 ml of chloroform was added. The mixture was shaken vigorously for 30 s, stored for 5 min at 4°C and centrifuged at 15 000 g for 15 min again. The supernatant was transferred and mixed with 0.5 μl of glycogen and 0.8 ml of isopropanol. After storage for >30 min at 4°C, the mixture was centrifuged at 15 000 g for 15 min at 4°C. The resultant supernatant was then carefully removed. The pellet containing RNA was washed with 70% ethanol three times, allowed to air-dry, and dissolved in 20 μl of RNase-free ddH_2O. The RNA concentration was determined by OD_{260}, measured by an ND-1000 Spectrophotometer® (NanoDrop, Wilmington, DE, USA). Approximately 40 ng of total RNA per sample was reverse transcripted in a 20 μl reaction using Transcriptor First Strand cDNA Synthesis Kit® (Roche, Basel, Switzerland) following the manufacturer's protocols.

PCR and sizing of PCR products

To compare the preserved length of mRNA between formalin-fixed and frozen samples, primers were designed using Primer 3 (http://frodo.wi.mit.edu/cgi-bin/primer3/primer3_www.cgi), on mRNA of *COCH* (accession no. NM004086), the coded protein of which is abundant in the inner ear [12]. Eight forward primers and one reverse primer were made to amplify 249–976 bp cDNA fragments (Figure 2). PCR was performed in a 20 μl volume containing 10 μl Premix Taq® (Takara Bio, Otsu, Japan), 0.5 μM of each specific primer and 1 μl of cDNA from the RT reaction. After initial incubation at 94°C for 3 min, the reaction mixtures were subjected to 35 cycles of amplification using the following sequence: 94°C for 30 s, 55°C for 30 s, and 72°C for 45 s. This was followed by a final extension step at 72°C for 7 min. Finally, 8 μl of the reaction mixture was run on a 2% agarose gel and visualized with ethidium bromide. Each amplification product was sequenced on an ABI PRISM® 3100 Genetic Analyzer (Applied Biosystems, Foster City, CA, USA).

Quantitative PCR analysis

To compare the quantity of mRNA for PCR level, quantitative real-time PCR was performed. TaqMan PCR® is a quantitative real-time PCR technique based on the 5′ exonuclease activity of TaqPolymerase [13]. In addition to the sense and antisense primers, a nonextendable oligonucleotide probe with